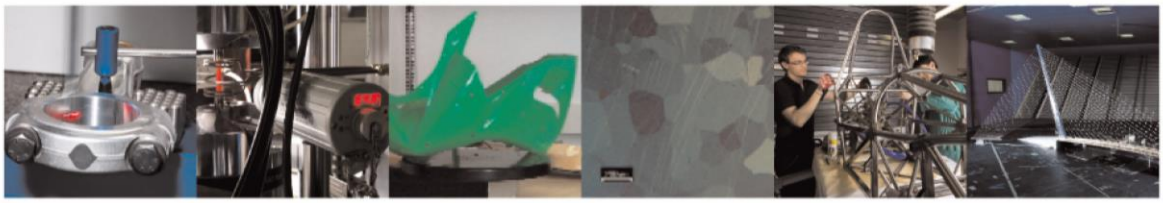

Comparative study between CW and PW emissions in selective laser melting

Caprio, Leonardo; Demir, Ali Gökhan; Previtali, Barbara

DIPARTIMENTO DI MECCANICA ■ POLITECNICO DI MILANO
via G. La Masa, 1 ■ 20156 Milano ■ EMAIL (PEC): pecmecc@cert.polimi.it
http://www.mecc.polimi.it
Rev. 0

COMPARATIVE STUDY BETWEEN CW AND PW EMISSIONS IN SELECTIVE LASER MELTING

Leonardo Caprio[1], Ali Gökhan Demir[1], Barbara Previtali[1]

[1] Department of Mechanical Engineering, Politecnico di Milano, Via La Masa 1, Milan, 20156, Italy

Abstract

The definition of process parameters depending on the geometry of the workpiece is one of the main challenges for Selective Laser Melting (SLM). The possibility to use different emission modes is an essential feature of the contemporary fiber lasers, which still requires further attention for controlling the melt pool size. Most of the commercially available SLM systems operates with continuous wave (CW) emission lasers. As a consequence, a substantial effort has been directed towards obtaining full densification by considering the variation of process parameters in CW modality. Pulsed wave (PW) emission achieved by power modulation of a fiber laser is preferred by a smaller fraction of the industrial SLM systems. The differences between the two emission regimes, advantages and disadvantages in their use have not been fully understood.

Accordingly, this work proposes a comparative study between the two emission regimes in SLM, namely PW and CW. For this purpose, a single mode fiber laser is coupled to a prototype SLM system composed of an automated powder-bed and a scanner head. The laser source is extensively characterized for pulsed wave emission characteristics in a power modulated regime. Conditions providing the same energy content over the single track were determined and their effect on single track densification is studied. High speed imaging (HSI) is used to observe the differences in the melt pool formation in situ. The overall results confirm that CW emission provides a larger and more stable molten pool during the process, resulting in higher deposition rates. On the other hand, under stable conditions, PW emission provides relatively narrow tracks, which might be problematic for porosity formation and at the same time useful for the production of fine geometries.

Introduction

Amongst the additive manufacturing field, the selective laser melting (SLM) technology has been identified as capable of concurring with conventional technologies in the manufacturing of mechanical components in terms of mechanical properties [1-3]. The choice of this powder bed fusion process is convenient with respect to traditional production methods when low batch production with high value materials and complex geometries is required. Process parameter optimization with the aim of minimizing porosity, reducing geometrical errors and increasing part accuracy has been conducted in numerous works[4-9]. The key process parameter for regulating these part quality indicators has been identified as fluence, which is the energy density delivered to the powder bed. Often the densification phenomenon and the underlying process dynamics have been studied using fluence and single track depositions [10-13]. Yadroitsev *et al.* were amongst the first to investigate these aspects with the aim of identifying ideal processing conditions for the realization of fine features while Li *et al.* investigated the balling phenomenon.

These studies were conducted using CW emission with active fiber laser sources, which are currently employed by the majority of commercially available SLM systems[14]. However, a smaller fraction of the available industrial systems prefers pulsed wave (PW) emission through modulation of the pumping media with kilohertz repetition levels. The reasons for the choice of different temporal emission modes are yet unclear amongst both the academic and industrial communities.

The aim of this study is therefore of understanding the differences in densification mechanisms between PW and CW emission modes in SLM. A model is presented to determine process parameters at equivalent energetic conditions for the realization of single tracks. An open SLM platform was used for this study, where a single-mode fiber laser was implemented. The laser source was extensively characterized in terms power modulation and the resultant pulse shape and temporal emission profiles. Subsequently, the experimental campaign at fixed energetic levels was conducted and specimens were characterized in terms of track width and volume of deposited material. High speed videos were registered on the same system to observe the process dynamics in-situ and identify the main differences in the melt pool dynamics during the SLM process. The results show that CW emission deposits a higher amount of

material and larger track width due to the greater melt pool dimensions depicted by HSI.

Modelling

PW emission results in an intermittent release of energy during the process. The use of power modulation for achieving PW emission results in the fast switching of the laser source, which results in long pulses with peak power similar to the maximum power at CW emission. Concerning the SLM process, a comparative analysis requires that at least the same amount of energy is released on the powder bed both with CW and PW emissions. With fixed power, temporal spacing of the pulses in PW emission, hence the scan speed has to be compensated.

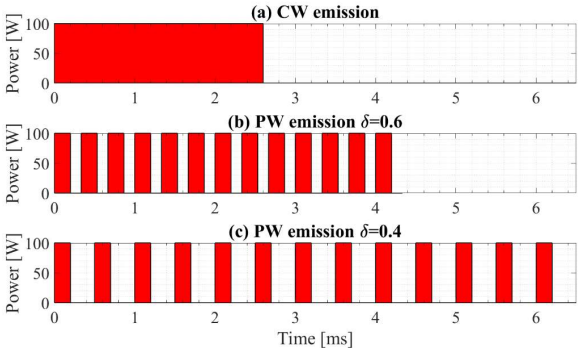

Figure 1 Temporal profile of different emission modes at constant energetic input with same peak power $P_{pk.}$ (a) CW, (b) PW with δ=0.6, (c) PW with δ=0.4

It is possible to formulate a model that defines process parameters for PW and CW emission regimes at fixed released energy levels during the SLM process. Concerning a single-track deposition, the energy input E_{line} [J] can be calculated as:

$$E_{line} = P_{avg} \cdot t_{line} \tag{1}$$

where P_{avg} [W] is the average power output delivered by the laser source and t_{line} [s] the period of time the laser beam takes to complete the line. If continuous wave emission regime is considered, it is possible to define:

$$E_{line\ CW} = P_{CW} \cdot t_{line\ CW} \tag{2}$$

where P_{CW} is the power delivered by CW laser emission and t_{lineCW} is:

$$t_{lineCW} = \frac{l}{v_{cw}} \tag{3}$$

where l [mm] is the length of the single track and v_{cw} [mm/s] is the scan speed during CW laser emission. Therefore, we can define:

$$E_{line\ CW} = \frac{P_{cw}}{v_{cw}} \cdot l \tag{4}$$

where $E_{line\ CW}$ [J] is the line energy of a track produced using CW laser emission.

Concerning the PW emission mode, the "on-the-fly" scanning mode is commonly used, which implies that the galvanometric mirrors are moving continuously while the laser is pulsating. Accordingly, the average power delivered by PW emission has to be taken into account (P_{avg} [W]), thus:

$$E_{line\ PW} = P_{avg} \cdot t_{line\ PW} \tag{5}$$

An important parameter related to the PW emission is the duty cycle, which is defined as:

$$\delta = t_{on} \cdot PRR \tag{6}$$

where t_{on} is the pulse duration and PRR is the pulse repetition rate. PRR can be further defined as:

$$PRR = \frac{1}{t_{on} + t_{off}} \tag{7}$$

where t_{off} is the laser off time between consecutive pulses. The lower values of duty cycle indicate a larger temporal spacing between consecutive pulses, while the duty cycle of CW emission is 1. In the hypothesis of using the "on-the-fly" scanning mechanism, we can define $t_{line\ PW}$ [s] as:

$$t_{line\ PW} = \frac{l}{v_{pw}} \tag{8}$$

where v_{pw} [mm/s] is the scan speed during PW laser emission. Hence,

$$E_{line\ PW} = \frac{P_{avg}}{v_{pw}} \cdot l \tag{9}$$

Equating $E_{line\ CW} = E_{line\ PW}$, by applying the condition of constant energy delivered per single track produced in PW and CW laser emission, it is possible to define the v_{pw} as:

$$v_{pw} = \frac{P_{avg}}{P_{cw}} \cdot v_{cw} \tag{10}$$

Using Equation (9) it is thus possible to calculate the scan speed required to transfer the same amount of

energy with PW and CW. In order to simplify the comparison of the different emission modes, the scan speed of CW emission has been taken as reference in this work. For each reference case, an equivalent scan speed for CW (v_{cwEQ}) is determined and tested with different PW emission.

Materials and methods

Material

Gas atomized AISI 316L stainless steel powders were used throughout the study (Cogne Acciai, Brescia, Italy). The particle size varied between 19.7 µm ($d_{0.1}$) and 44.6 µm ($d_{0.9}$) with the average at 29.8 µm. The tap density was 5 g/cm^3, whereas the nominal material density is 8.1 g/cm^3.

Prototype SLM system

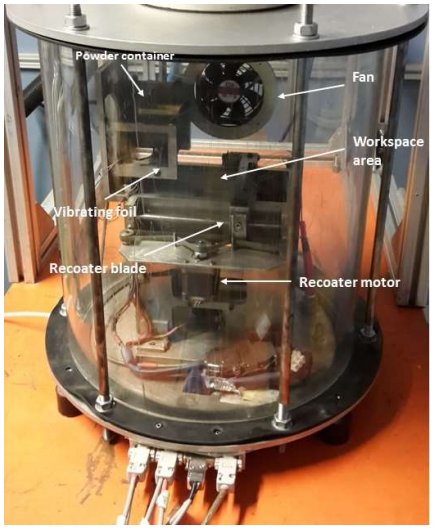

Figure 2 Image of the SLM prototype system

An in-house developed prototype SLM system (shown in Figure 2), namely Powderful, was employed throughout the study. A complete automation of the powder bed was implemented. The control of the system was conducted in a LabView environment (National Instruments, Austin, TX, USA).

The open set-up of the system allowed for operating both in controlled atmosphere and open chamber. In the case of processing in closed chamber configuration, a vacuum was applied down to 50 mbar of pressure first, and then argon gas was introduced. This procedure was repeated 3 times.

Optical chain and laser source

A single mode active fiber laser source, which could operate both in CW and PW emission (IPG Photonics YLR-150/750-QCW-AC, Cambridge, MA, USA), was used in the experimentation. The laser beam was coupled to a scanner head (El.En. Scan Fiber, Florence, Italy) and the scan path trajectory was designed using LogoTag software (Taglio, Piobesi d'Alba, Italy). The optical chain consisted in a 60 mm collimating lens and a 255 mm f-theta lens, resulting in a theoretical beam diameter of 55 µm on the focal plane.

The laser source was extensively characterized in terms of temporal emission modes and average power output during PW and CW emission modes using a power meter (Laserpoint W-3000-D55-HPB-RS, Vimodrone, Italy). The diode pumping current is the main parameter used to set the power level. Pulse duration and duty cycle could be set via a trigger signal. During CW emission, maximum output power (at 100 % diode pumping current) resulted being P_{cw}=244 W. The pulse temporal profiles were acquired using a fast photodiode at the maximum pumping current level (Thorlabs FGA10 InGaAs, Newton, NJ, USA). Duty cycles and pulse durations were commanded through the trigger signal. Seven levels of duty cycle between 0.2 and 0.8 and 3 levels of pulse duration between 100 and 200 µs were tested. Average power of all the tested conditions was measured. Pulse energy was calculated using the following expression:

$$E_{pulse} = P_{avg}/PRR \quad (11)$$

The photodiode output in voltage was converted to a power profile by a numerical derivation using the average pulse energy.

Table 1 Factors varied to characterize power temporal profiles during PW emission

Fixed factors	**Levels**
Diode pumping current, PI [%]	100
Variable factors	**Levels**
Duty cycle, δ	0.2; 0.3; 0.4; 0.5; 0.6; 0.7; 0.8
Pulse duration, t_{on} [µs]	100; 150; 200

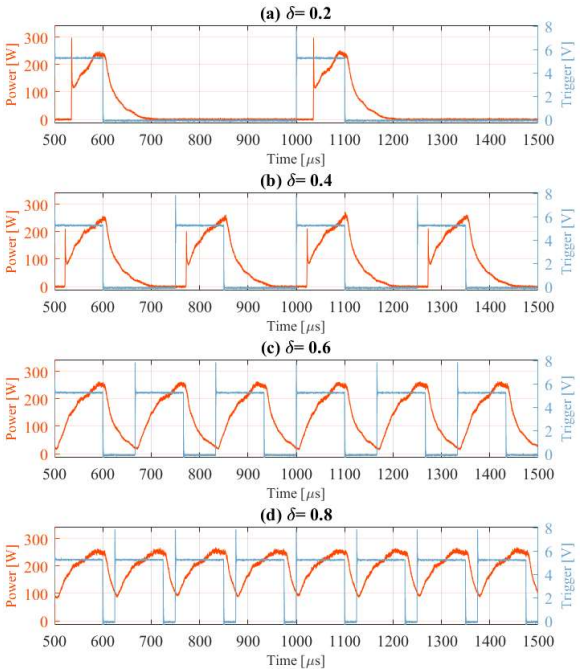

Figure 3 Pulse temporal shapes during PW emission. Effect of duty cycle (at fixed value of pulse duration t_{on}=100 µs). (a) δ=0.2, (b) δ=0.4, (c) δ=0.6, (d) δ=0.8. Trigger signal commanding diode pumping current in blue, power temporal profile in red.

In Figure 3, the effect of duty cycle on the temporal emission modes is shown. Increase in δ implies a reduction of t_{off}. Since the laser source employed in this work has non-negligible fall times greater than the latter parameter, this results in an almost-continuous emission at high values of duty cycle. Hence, in order to achieve a pulsed wave emission with an effective power variation, it is mandatory to use a maximum duty cycle of δ=0.6.

Furthermore, both in Figure 3 and Figure 4 it is possible to view the presence of significant rise times in the laser emission. This aspect is independent of the duty cycle parameter whereas a minimum pulse duration of 100 µs is required to reach a peak power emission equivalent to the maximum power output during CW emission. Further increases in the pulse duration imply a longer emission maximum output power emission values whilst the fall time of the laser emission is not affected by this parameter.

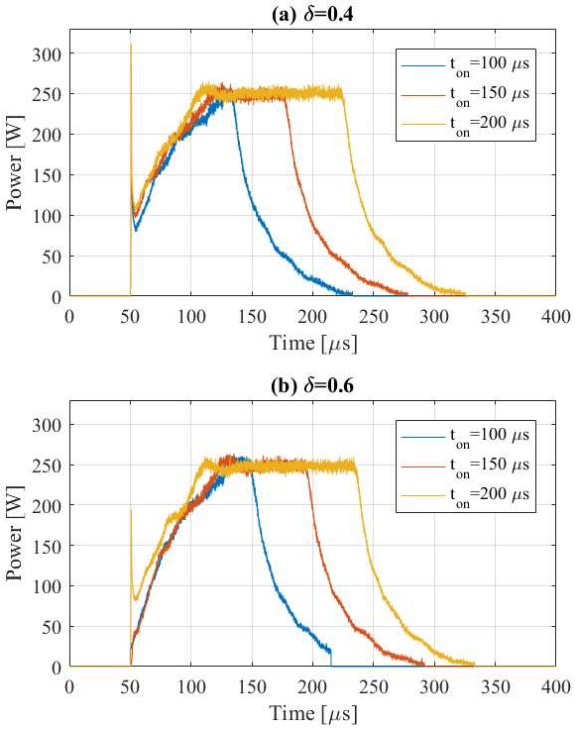

Figure 4 Pulse temporal shapes during PW emission. Effect of pulse duration at different levels of duty cycle (a) δ=0.4, (b) δ=0.6.

High Speed Imaging

The realization of single tracks during the SLM process was also observed by means of a high-speed camera with maximum acquisition rate of 900 000 fps, namely FASTCAM Mini AX 200 (Photron, Tokyo, Japan). The CAVILUX HF laser source (Cavitar, Tampere, Finland) was synchronized with the camera shutter speed for high speed illumination of the area of interest. Schematic representation of the experimental set-up for the HSI observations is shown in Figure 5. Videos were acquired at 30000 fps with a resolution of 512x384 pixels to observe the effect of the emission modes and 512x288 pixels to view the process at different levels of equivalent scanning speed, thus resulting in two different fields of view (estimated respectively as 2.20x1.65 mm^2 and 5.43x3.05 mm^2).

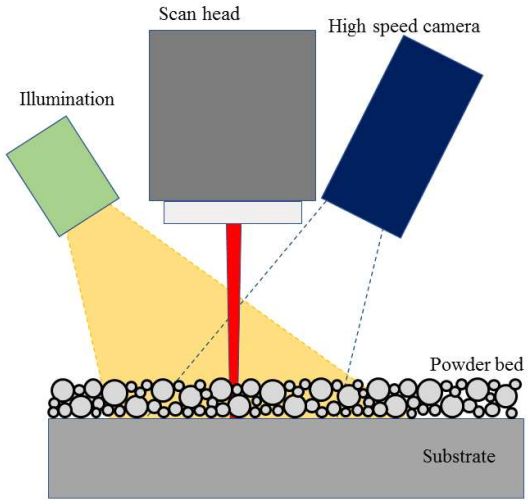

Figure 5 Schematic representation of the HSI set-up

Single track characterization

Single tracks realized in the experimental campaign were characterized in terms of track volume (V),mean width (w) and mean height (h). Measurements were done using focus variation microscopy (Infinite Focus from Alicona, Graz, Austria). Acquisitions were made on an area of 30x55 mm^2 with 5X objective on the scan plane. Estimated lateral and vertical resolutions were 7 µm and 0.5 µm respectively.

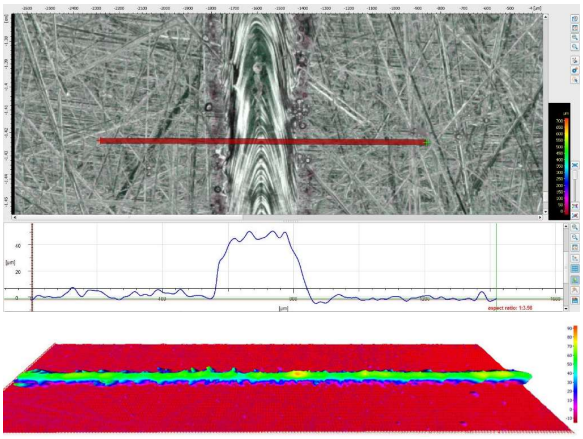

Figure 6 Example of track width and volume measurements of a single track.

Experimental plan

CW and PW emission modes were compared at fixed peak power levels produced with the maximum pump current level. Layer thickness was fixed at 50 µm, which is conventionally used for AISI 316L[15-17]. Focal point was set at the powder bed surface. Through preliminary experiments, stable processing conditions with CW emission were identified at scanning speeds between 50 and 450 mm/s. Accordingly, equivalent scan speed levels were fixed at 50, 250, and 450 mm/s. PW emission was tested at different levels of duty (0.4-0.6) and pulse duration (100-200 µs), in order to better comprehend the effect of temporal spacing of the pulses. Experiments were carried out under Ar. The fixed and varied factors during the realization of single tracks are indicated in Table 2. Each experimental condition was replicated four times.

Table 2 Fixed and varied factors for HSI process observation for CW and PW emission single tracks

Fixed factors	**Value**
Single track length, l [mm]	30
Layer thickness, t [µm]	50
Diode pumping current, PI [%]	100
Peak power, P_{pk} [W]	244
Focal position, Δz [mm]	0
Variable factors CW emission	**Value**
Scan speed, v_{cw} [mm/s]	50; 250; 450
Variable factors PW emission	**Value**
Scan speed, v_{cwEQ} [mm/s]	50; 250; 450
Duty cycle, δ	0.4; 0.6
Pulse duration, t_{on} [µs]	100; 200

Results

High Speed Imaging observations

High speed imaging observation of the process was done for each experimental condition with the off-axis configuration previously indicated.

Effect of scanning speed

Figure 7 compares the images obtained at different scan speeds using CW emission. At lower values of scan speed the melt pool is notably wider. As the energetic scan speed is increased, the melt pool elongates. Rather than a more effective heat transfer along the scan trajectory, this is expected to be due to a more limited heat transfer in the powder bed depth.

With reference to the particle motion surrounding the melt pool, at higher values of scan speed, advancement of the laser beam is faster than the particle motion therefore the phenomenon is more contained. The smaller interaction time of the laser beam with the

powder bed with greater scan speed affects the melt pool dynamics and results in a smaller denudation effect and suction of neighboring particles. Nonetheless, an excessive increase in terms of scan speed generates a balling phenomenon therefore a balance between the two conditions must be considered.

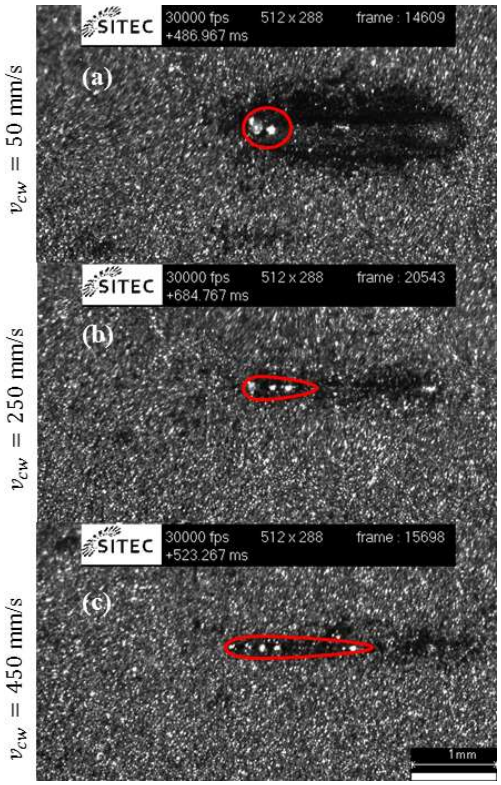

Figure 7 High speed images of the melt pool during the SLM process with CW emission at different levels of scan speed (contour indicated in red). (a) v_{cw}=50 mm/s; (b) v_{cw}=250 mm/s; (c) v_{cw}=450 mm/s

Effect of emission modes

The variation of the temporal emission modes greatly affects the melt pool dimension and its behavior. As shown in Figure 8, the melt pool is effectively larger and longer during CW emission. The HSI videos also depict an intermittent behavior in the melt pool dynamics when PW emission is employed. The effect of pulse duration on the melt pool dimension when observing the HSI videos on the other hand is less evident and does not sensibly affect the length and width of the melt pool. If we consider CW emission as effectively having a unitary value of duty cycle (δ=1), we can state that the melt pool stability increases with increasing values of duty cycle and is notably wider.

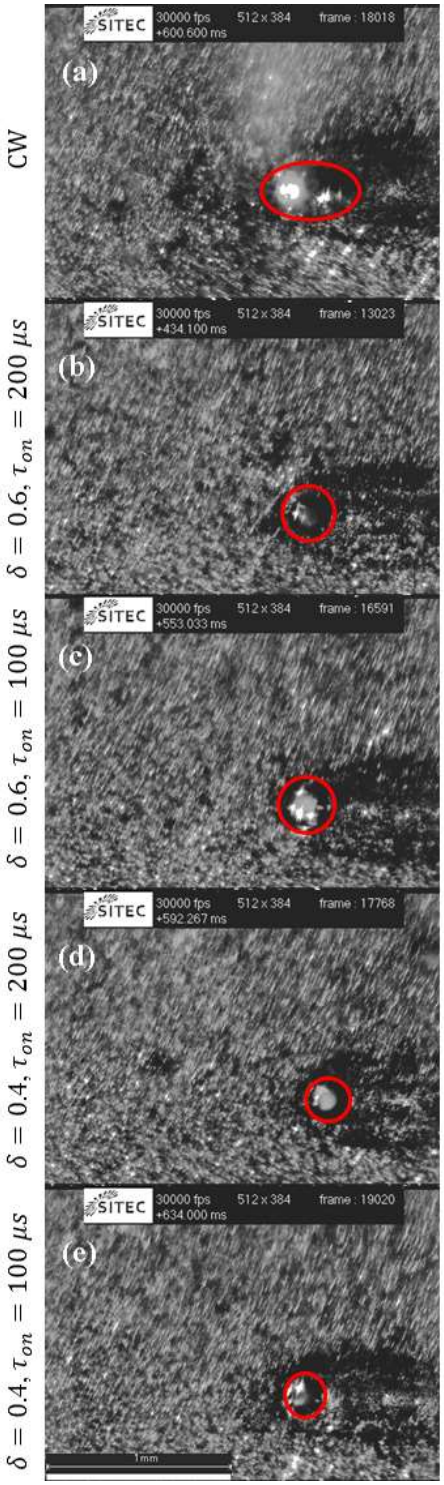

Figure 8 HSI of the SLM process at constant v_{cwEQ}=50 mm/s showing effect of emission modes on melt pool dimension (contour indicated in red).

The particle motion in proximity with the melt pool is a relevant phenomenon that could be observed with high

speed imaging. With CW emission, the majority of the gas atomized particles in the surrounding of the melt pool area tended to be attracted towards its center whilst a few were ejected possibly due to the formation of metallic vapor. This effect was much less evident with PW emission, due to the narrower melt pool, thus resulting also in a smaller denudation effect in the surrounding melt pool area.

Track width

The qualitative observations of the high-speed imaging acquisitions were confirmed by the track width measurements (shown in Figure 9), which can thus be considered as representative of the melt pool width. A significant increase in terms of track width with different emission modes can be noted. Furthermore, at lower energetic input values (i.e. higher values of equivalent scan speed) there is a decrease in terms of track width, representative of the melt pool restriction in these operating conditions. On the other hand, within the same equivalent speed conditions, differences in the temporal characteristics of the pulses related to duty and pulse duration appear to be insignificant.

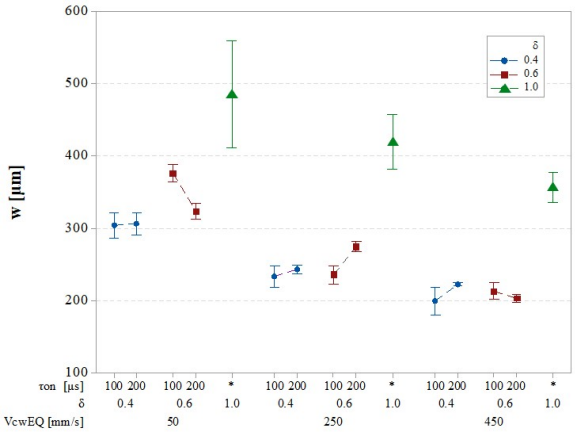

Figure 9 Track width with respect to process parameters. Error bars represent standard error.

Volume of deposited material

Analogously to the track width, the volume of deposited material is coherent with the HSI observations. As previously illustrated, increasing the duty cycle (culminating with CW emission with δ=1) results in a clear increase in terms of deposited volume, possibly due to the greater melt pool dimensions, higher stability and increased suction of neighboring particles. The melt pool elongation and restriction at higher levels of equivalent scanning speed, on the other hand, can be seen as the reason for the lower volumetric deposition at lower energetic input levels.

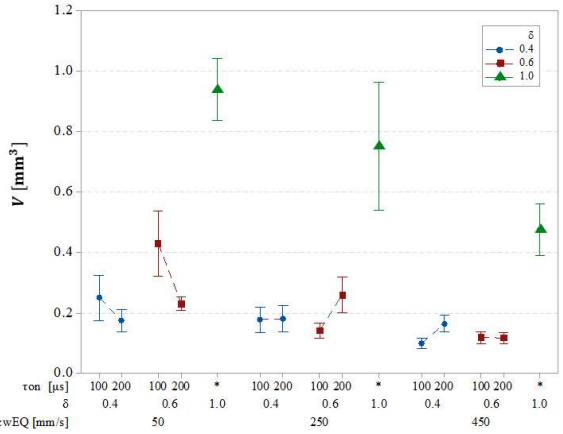

Figure 10 Volume of deposited material with respect to process parameters. Error bars represent standard error.

Aspect ratio

Variations in terms of track height with respect to process parameters were analogous to those of track width. CW emission allowed for higher aspect ratio deposition (as shown in Figure 11) thus underlining the effect of different temporal emission modes on melt pool geometry and solidification phenomena whereas smaller changes were denoted at different equivalent scanning speed values.

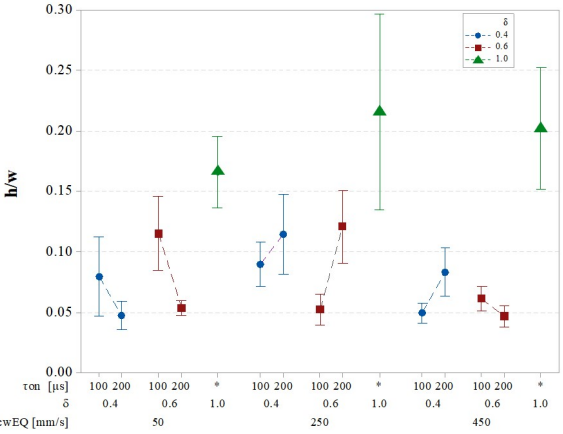

Figure 11 Track aspect ratio (*h/w*) with respect to process parameters. Error bars represent standard error.

Discussion

The results of the current study evidence a significant difference in the densification behavior of the powder bed under the effect of different temporal emission

modes. The in-situ process diagnosis through high speed imaging allowed for a descriptive analysis of the phenomena occurring during the process. A strong correspondence between emission modes and melt pool dynamics was evinced and this aspect reflects in the part quality indicators, namely track width and volume of deposited material. Previous studies using meso-scale simulation models identify an important link between the laser radiation interaction with randomly packed powder beds and melt pool dynamics[18-20], confirming these observations. Furthermore, according to the simulations, the strong Marangoni forces generated by elevated surface tension and steep temperature difference between the melt area and the neighboring powder bed determines the lack of particles near the single-track formation (i.e. the particle suction previously denoted)[19]. Furthermore, the presence of recoil pressure in the simulations generates the spattering effect which was also observed in the present work[19].

As the experimental results depict, an increase in process resolution (i.e. reduced track width) can obtained by employing PW emission which yields a smaller, more contained melt pool. This effect might be related to a less efficient heat transfer mechanism generated by a lower optical coupling between the powder bed and laser light. Possibly, a result of this phenomenon is linked with the higher volumetric deposition with CW emission. In order to explain the underlying physics of the process it often useful to refer to analogous processes to SLM and is the case of laser [21]. According to Assuncao *et al.*, it is possible to identify the output difference between PW and CW emission in a variation of the interaction time with a specific point which modifies the keyhole formation during the process [22]. Yet it is not possible to confirm the presence of plasma in the high speed imaging observations and is hence opportune to refer to models specifically developed to represent the laser powder interaction of the SLM process.

In literature, it is commonly accepted to model the process during CW emission as a volumetric heat source due to the multiple reflections of the emission radiation within the powder bed[23,24]. However, no study exists describing the different physical phenomena underlying the laser-powder interaction due to different temporal emission modes. It therefore stands out as a relevant question whether a variation in the emission regime affects this aspect and can be taken as a starting point for future developments of the present work.

Overall, it may be stated that the choice of the emission regime should be made depending on the workpiece geometry. For bulk areas, where a higher volumetric deposition rate is required, CW emission is preferable whereas the use of PW emission is advantageous in the realization of finer geometries, requiring greater precision.

Conclusions

The present investigation compares the effect of different temporal emission modes during the SLM process. The laser source used in the experimentation was characterized in terms of emission profiles and power output to define the emission radiation. Successively, an experimental campaign comparing single tracks realized at fixed energetic deposition values was conducted.

Results show increases in deposited volume up to three times with CW emission with respect to pulsed wave although this also coincides with a significant increase in terms of track width. Therefore, with the aim of a higher process resolution it would be helpful to employ power modulation of the laser source whereas higher amounts of volume may be deposited with continuous wave emission.

Process diagnosis, through high speed imaging observations of each experimental condition, relates these results to the melt pool dynamics. Melt pool elongation was observable at increasing levels of scanning speed. CW emission determines a higher melt pool stability, larger and longer with respect to PW, thus yielding a higher deposition of the material.

Acknowledgments

This work was supported by Regione Lombardia under the call “Creatività: Eventi e Luoghi per L’innovazione nella Moda e nel Design, Linea 2: Infrastrutturazione Fisica e Digitale” and the project MADE4LO under the call "POR FESR 2014-2020 ASSE I - AZIONE I.1.B.1.3”. The project presented in this paper has been supported by the Autonomous Province of Trento, Italy, through the Regional Law 6/98. Name of the granted Project: LT4.0.

The authors would like to acknowledge BLM Group for the technical support and hardware for high speed imaging acquisitions. ElEn and Taglio are acknowledged for their technical support. IPG Photonics Italy is acknowledged for the laser loan.

References

[1] Yap C, Chua C, Dong Z, Liu Z, Zhang D, Loh L, et al. (2015) Review of selective laser melting: Materials

and applications. Applied Physics Reviews ;2(4):041101.

[2] Santos EC, Shiomi M, Osakada K, Laoui T. (2006) Rapid manufacturing of metal components by laser forming. Int J Mach Tools Manuf ;46(12):1459-1468.

[3] Gibson I, Rosen DW, Stucker B. Additive manufacturing technologies. : Springer; 2010.

[4] Read N, Wang W, Essa K, Attallah MM. (2015) Selective laser melting of AlSi10Mg alloy: Process optimisation and mechanical properties development. Materials & Design (1980-2015) ;65:417-424.

[5] Bagheri ZS, Melancon D, Liu L, Johnston RB, Pasini D. (2017) Compensation strategy to reduce geometry and mechanics mismatches in porous biomaterials built with Selective Laser Melting. Journal of the mechanical behavior of biomedical materials ;70:17-27.

[6] Strano G, Hao L, Everson RM, Evans KE. (2013) Surface roughness analysis, modelling and prediction in selective laser melting. J Mater Process Technol ;213(4):589-597.

[7] Zhang B, Dembinski L, Coddet C. (2013) The study of the laser parameters and environment variables effect on mechanical properties of high compact parts elaborated by selective laser melting 316L powder. Materials Science and Engineering: A ;584:21-31.

[8] Zhang B, Coddet C. (2016) Selective laser melting of iron powder: observation of melting mechanism and densification behavior via point-track-surface-part research. Journal of Manufacturing Science and Engineering ;138(5):051001.

[9] Vandenbroucke B, Jean-Pierre Kruth. (2007) Selective laser melting of biocompatible metals for rapid manufacturing of medical parts. Rapid Prototyping Journal 08/07; 2015/12;13(4):196-203.

[10] Yadroitsev I, Shishkovsky I, Bertrand P, Smurov I. (2009) Manufacturing of fine-structured 3D porous filter elements by selective laser melting. Appl Surf Sci ;255(10):5523-5527.

[11] Li R, Liu J, Shi Y, Wang L, Jiang W. (2012) Balling behavior of stainless steel and nickel powder during selective laser melting process. The International Journal of Advanced Manufacturing Technology ;59(9-12):1025-1035.

[12] Yadroitsev I, Bertrand P, Smurov I. (2007) Parametric analysis of the selective laser melting process. Appl Surf Sci 7/31;253(19):8064-8069.

[13] Yadroitsev I, Yadroitsava I, Bertrand P, Smurov I. (2012) Factor analysis of selective laser melting process parameters and geometrical characteristics of synthesized single tracks. Rapid Prototyping Journal ;18(3):201-208.

[14] Demir AG, Colombo P, Previtali B. (2017) From pulsed to continuous wave emission in SLM with contemporary fiber laser sources: effect of temporal and spatial pulse overlap in part quality. The International Journal of Advanced Manufacturing Technology :1-14.

[15] Cherry J, Davies H, Mehmood S, Lavery N, Brown S, Sienz J. (2015) Investigation into the effect of process parameters on microstructural and physical properties of 316L stainless steel parts by selective laser melting. The International Journal of Advanced Manufacturing Technology ;76(5-8):869-879.

[16] Investigation the effect of particle size distribution on processing parameters optimisation in selective laser melting process. International solid freeform fabrication symposium: an additive manufacturing conference. University of Texas at Austin, Austin; 2011.

[17] Sun Z, Tan X, Tor SB, Yeong WY. (2016) Selective laser melting of stainless steel 316L with low porosity and high build rates. Mater Des ;104:197-204.

[18] Khairallah SA, Anderson A. (2014) Mesoscopic simulation model of selective laser melting of stainless steel powder. J Mater Process Technol ;214(11):2627-2636.

[19] Khairallah SA, Anderson AT, Rubenchik A, King WE. (2016) Laser powder-bed fusion additive manufacturing: physics of complex melt flow and formation mechanisms of pores, spatter, and denudation zones. Acta Materialia ;108:36-45.

[20] Xia M, Gu D, Yu G, Dai D, Chen H, Shi Q. (2017) Porosity evolution and its thermodynamic mechanism of randomly packed powder-bed during selective laser melting of Inconel 718 alloy. Int J Mach Tools Manuf ;116:96-106.

[21] A review of thermal analysis methods in Laser Sintering and Selective Laser Melting. Proceedings of Solid Freeform Fabrication Symposium Austin, TX; 2012.

[22] Assuncao E, Williams S. (2013) Comparison of continuous wave and pulsed wave laser welding effects. Optics and Lasers in Engineering ;51(6):674-680.

[23] Wang X, Laoui T, Bonse J, Kruth J, Lauwers B, Froyen L. (2002) Direct selective laser sintering of hard metal powders: experimental study and simulation. The International Journal of Advanced Manufacturing Technology ;19(5):351-357.

[24] Gusarov A, Yadroitsev I, Bertrand P, Smurov I. (2009) Model of radiation and heat transfer in laser-powder interaction zone at selective laser melting. Journal of heat transfer ;131(7):072101.

Meet the Authors

Leonardo Caprio was born in 1993 and graduated in Mechanical Engineering with specialisation in Advanced Materials and Manufacturing from the Politecnico di Milano in 2017. His research is currently focused on the Selective Laser Melting technology in the field of Additive Manufacturing at the AddMe.Lab of the Politecnico di Milano.

Ali Gökhan Demir was born in Istanbul, Turkey, in 1985. He received the M.Sc. degree in mechanical engineering and European Ph.D. degree in mechanical engineering from the Politecnico di Milano, Italy, in 2009 and 2014, respectively. He has been Assistant Professor with the department of Mechanical Engineering, Politecnico di Milano, since 2015. He has authored over 50 papers in international journals and international conference proceedings. His current research interests include laser-based manufacturing processes, mainly, additive manufacturing, laser micromachining, and process monitoring with the SITEC - Laboratory for Laser Applications.

Barbara Previtali received the Ph.D. degree in manufacturing and production system from the Politecnico di Milano, Milan, Italy, in 2002. In 2016, she was appointed as Full Professor in the Mechanical Engineering Department, Politecnico di Milano. She leads the SITEC—Laboratory for Laser Applications and PromozioneL@ser with AITeM, which collects Italian laser users in industry and academia. Her current research interests include modeling, optimization and control of laser processes in their application in various fields. On these research subjects, she has authored or co-authored over 100 papers in refereed international journals and international conferences and two international patents.